Using pressure transients within a polymeric membrane for gas composition measurements

Sofia De Gregorio*, Marco Camarda, Santo Cappuzzo, Sergio Gurrieri

Istituto Nazionale di Geofisica e Vulcanologia, sezione di Palermo, via Ugo La Malfa 153, 90146 Palermo, Italy

*Corresponding author: E-mail: s.degregorio@pa.ingv.it Tel: +390916809439 Fax: +390916809449

Abstract

The properties of polymeric membranes and measurements of gas concentrations are common elements of industrial processes and scientific research. Here we report a methodology whereby pressure measurements inside a closed polymeric membrane tube can be quantitatively related to the composition of the external gas. This approach is founded on the different rates at which the gases permeate into and out of the interior of the polymeric tube. The difference between the amounts of gas entering and leaving the tube triggers a pressure transient. The features of this transient depend on the species of the involved gases and their partial pressures and under certain conditions, allow the concentration of one or more species to be estimated. We outline the theoretical principles behind the proposed methodology and conduct laboratory tests on a device that could be adaptable to continuous measurements of CO_2 partial pressure in field applications.

Keywords: gas concentration measurements, polymeric membranes, continuous monitoring, carbon dioxide

1. Introduction

Measurements of gas concentration are useful in industrial applications and many fields of science, including geochemistry, oceanography, and volcano monitoring, [e.g., *D'Alessandro et al*., 1997 and *Beaubien et al.*, 2003; *Capasso et al*., 2005; *Lupton et al.*, 2006; *Shinohara et al*., 2008; *Fischer, et al.*, 2009]. Many measurement methods employ polymeric membranes [*Kana et al.*, 1994; *Takahata et al.*, 1997; *Tortell*, 2005], generally requiring an instrument that records an electrical current or voltage proportional to the amount of gas molecules, which are selected or separated from a gas mixture using devices such as vacuum pumps, electromagnets, and chromatograph columns. In almost all such devices, the gas mixture is introduced inside the instrument, making it vulnerable to damage by corrosive gas species or liquid water; consequently, these instruments can be used, with difficulty, in environments in which sulphur or acid species are present or in which powerful vapour fluxes and steam condensation phenomena occur. Unfortunately, such environments are commonly those that promote the discharge of fluids from natural systems, making them the best sites at which to conduct measurements as part of environmental surveillance programs. These extreme conditions can be encountered in fumarole fields of active volcano. The employ of common *insitu* instruments (e.g. infrared spectrophotometer and gas chromatograph), in these areas, requests the use of complex apparatus in order to preserve the instruments from vapour and corrosive gases. Further, technical problems can occurred, regarding: the power supply; the stability of optical sensor; the block of gas pipe for sulphur deposition [*Faber et al.*, 2003] or block of the valves by aerosols of sublimates precipitation [*Zimmer et al.*, 2003].

The method, presented in this paper, measures gas concentrations using only a pressure transducer, which results in low power requirements and a robust instrument easily transportable. These features confer to the presented method, among the others, the advantage to be used, without difficulty, in extreme environments.

2. Theoretical Principles

The proposed methodology is based on gas transport through a polymeric membrane, as described by the solution–diffusion model [*Barrer*, 1934; *Wijmans and Baker*, 1995], according to which the gas on the high-pressure side of the membrane dissolves into the membrane body and diffuses toward the low-pressure side, where the gas is finally desorbed. The law governing the flux through the membrane is

$$J_i = Kp\frac{\Delta P}{h} \quad (1)$$

where J_i is the flux, Kp is the permeability coefficient, ΔP is the pressure difference, and h is membrane thickness. As shown in Equation (1), the amount of permeating gas is proportional to the pressure gradient across the membrane, and the Kp coefficient. In exchange processes between gas within a closed tube of polymeric membrane and the external atmosphere, the gas flux has two principal directions (i.e., inward and outward), in response to the gas partial pressure difference between the inner of tube and external atmosphere. E.g., if the partial pressure of a given gas is higher in the atmosphere the gas will move towards the inner of the tube (inward flux).

For a given membrane, the Kp value of gases shows variations of up to an order of magnitude [*Scholes et al.*, 2008]. A large difference in Kp value between that for the gas inside and outside the membrane produces a pronounced disparity between the amount of gas entering and leaving the tube, resulting in turn in a marked change in the number of molecules in the headspace of the polymeric tube, and a transient in the internal pressure.

According to Equation (1), the feature of the transient, for a given membrane, depends on the gas species and their partial pressure.

3. Results and Discussion

On this basis, we developed a new methodology to determine the gas concentrations by measuring the temporal variation in total pressure (P_t) within a polymeric tube. We started with an equation that describes temporal variations in the partial pressure of a single gas [*De Gregorio et al*., 2005]

$$P_i(t) = P_a + (P_{in} - P_a)\exp\left(-\frac{Kp \cdot A}{Vh}t\right) \quad (2)$$

where $P_i(t)$ is the partial pressure of the *i*th gas at time *t*, P_a is the equilibrium partial pressure of the *i*th gas, P_{in} is the initial partial pressure of the *i*th gas inside the tube, *Kp* is the permeation coefficient, *A* is the area of the membrane surface, *V* is the internal volume of the tube, and *h* is membrane thickness. As shown in equation (2), the variation in partial pressure of each gas depends on the initial partial pressure within the tube and the equilibrium partial pressure, which represents the partial pressure of the gas in the environment surrounding the tube.

Considering that the total pressure of a gas mixture is given by the summation of individual partial pressures, temporal variations in P_t can be obtained from the sum of variations in individual $P_i(t)$ values; i.e., from the sum of *n* equations such as Equation (2). For a bicomponent system consisting of a mixture of Gas 1 and Gas 2, temporal variations in P_t can be described as

$$P_t(t) = P_{a1} + (P_{in1} - P_{a1})\exp\left(-\frac{Kp_1 \cdot A}{Vh}t\right) + P_{a2} + (P_{in2} - P_{a2})\exp\left(-\frac{Kp_2 \cdot A}{Vh}t\right) \quad (3)$$

Assuming that at initial state the value of P_t inside the tube is equal to the pressure in the surrounding atmosphere (P_{atm}), we have $P_{in1} + P_{in2} = P_{atm}$ and $P_{a2} + P_{a1} = P_{atm}$. Equation (3) then becomes

$$P_t(t) = P_{atm} + (P_{a2} - P_{in2})\left[\exp\left(-\frac{Kp_1 \cdot A}{Vh}t\right) - \exp\left(-\frac{Kp_2 \cdot A}{Vh}t\right)\right] \quad (4)$$

If $P_{a2} \neq P_{in2}$, then $P_t(t)$ changes with time until $P_{a2} = P_{in2}$; Figure 1 shows theoretical curves of temporal variations in P_t, as calculated using Equation (4) and considering four values of $(P_{a2} - P_{in2})$. The upper part of the figure considers $Kp_1 < Kp_2$; in this condition, gas 2 is able to permeate inside the tube faster than is gas 1, resulting in an increase in P_t. In contrast, for $Kp_1 > Kp_2$ (lower part of the figure) we observe a decrease in P_t. Nevertheless, in both cases the rate of variation in P_t is initially proportional to $(P_{a2} - P_{in2})$. The relationship between the rate of P_t variation and $(P_{a2} - P_{in2})$ is given by the first derivative of Equation (4) at $t = 0$:

$$\left(\frac{\partial P_t(t)}{\partial t}\right)_{t=0} = \frac{A}{Vh}(Kp_2 - Kp_1)(P_{a2} - P_{in2}) \quad (5)$$

Equation (5) can be used to compute the gas partial pressure based on measurements of temporal variations in P_t within a polymeric tube, provided we know the geometric characteristics of the system A/Vh and the Kp values of the involved gases. The geometric features can be measured directly, and the Kp values of many gases for the most common membranes are reported in the literature. Otherwise, the term $A/Vh(Kp_2-Kp_1)$ can be determined experimentally by calculating $[(\partial P_t/\partial t)_{t=0}]$ for different $(P_{a2} - P_{in2})$ values and computing the angular coefficient of the straight line fitting the obtained values. The values of gas

concentration are easily obtained from the computed partial pressure (P_a) and the total pressure of the environment (P_T), in agreement with Dalton's Law: $P_a / P_T = Xi$, where Xi is the molar fraction.

To verify the validity of the proposed methodology, we undertook a case study and performed numerous experiments. In the case study, a polymeric membrane tube was filled with atmospheric gases; the external atmosphere consisted of atmospheric gases (O_2 and N_2 have a constant ratio afterwards they can be considered as a single gases, Gas 1) and CO_2 (Gas 2). We selected this example because the measurement of CO_2 concentrations in the atmosphere has many scientific implications; e.g.: volcano surveillance, studies of gas hazards and greenhouse gases [*Aiuppa et al.*, 2008; *Zhang et al*., 2008].

In the experiments, we used a polytetrafluroethylene (PTFE) membrane because the *Kp* value of CO_2 (Kp_{CO2}=28 Barrer [*De Gregorio et al.*, 2005]) for this membrane is an order of magnitude greater than that of atmospheric gases (Kp_{N2}=4 Barrer Kp_{O2}=7 Barrer [*De Gregorio et al.*, 2005]), thereby ensuring a detectable transient pressure. Further, the PTFE has a good stiffness and can bear pressure variation without significantly deformation.

All the tests were performed in a steel cylinder within which it was possible to create a controlled atmosphere (Figure 2). Inside the cylinder, the PTFE tube (5 m long and with wall thickness of 0.0003 m) was connected to two capillaries located on the cylinder's plug. To the external part of the capillaries was connected a closed circuit, with pressure transducers (Freescale MPX2100AP with 12V DC supply), a pump, and two electrovalves. Prior to each test, the tube was filled with air at atmospheric pressure, during which time the pump was operated for 2 minutes with the two electrovalves open; the valves were then closed and the measurements begun. The sampling sequence was automated using a tailor-made electronic device. Total pressure (P_t) inside the PTFE tube was measured to an accuracy of ± 0.0001 atm. The cylinder was provided of additional pressure transducer for measuring the total pressure

144 inside it (Figure 2). For all test, samples of gas were collected from the cylinder by the
145 sampling valve (Figure 2), using a syringe, three-way stopcock and a sample holder. The
146 samples were introduced to a gas chromatograph (GC) Perkin - Elmer Clarus 500, equipped
147 with column Packed 60/80 Carboxen 1000, hot wire and flame ionization detectors; Ar was the
148 carrier gas, the analysis had a precision of ± 3%. The equilibrium partial pressure (P_a) values
149 were obtained by multiplying the concentrations measured with the GC by the mean values of
150 pressure recorded inside the cylinder. Experiments were performed for eight different CO_2
151 partial pressures (P_a), 10 series for each. In each series, P_t inside the PTFE tube was measured
152 at 30-second intervals over 10 minutes. The series were repeated every 3 hours to ensure the
153 being of no perturbation conditions. During the series no relevant pressure variations were
154 recorded inside the cylinder.

155 As an example, Figure 3 shows a series for each CO_2 partial pressure (the data of all the
156 series are reported in supplementary material), as predicted by the model, the slopes of the
157 initial parts of the curves are proportional to CO_2 partial pressure. The slopes of the curves at
158 t=0 are given by the angular coefficients of the tangents to the curves i.e. $[(\partial P_t/\partial t)_{t=0}]$, these
159 values can be used, according to equation (5), to calculate CO_2 partial pressures. The value of
160 $[(\partial P_t/\partial t)_{t=0}]$ can be obtained fitting a function to experimental data and computing its first
161 derivative a t=0. The CO_2 concentrations can be easily obtained according to Dalton's Law by
162 measurements of the total pressure.

163 Among the diverse functions available for fitting the experimental data, we chose a five-
164 degree polynomial function, because it fitted to the data very well (Figure 3) and allowed us a
165 fast computation of the value of $[(\partial P_t/\partial t)_{t=0}]$, given that, it is the first-degree term of the
166 polynomial function. The computed values for every series are listed in Table 1, along with
167 statistical parameters. As expected, the value of $[(\partial P_t/\partial t)_{t=0}]$ increases with increasing CO_2
168 within the cylinder. The mean value varies from $1.21 \cdot 10^5$ atm sec^{-1} for the series with the

lowest partial pressure of CO_2 (0.032 atm) to $36.78 \cdot 10^5$ atm sec^{-1} for the series with the highest (0.89 atm). The methodology yields reproducible results (uncertainty between $0.07 \cdot 10^5$ and $0.26 \cdot 10^5$ atm sec^{-1}) and has good precision ($\leq$ 6%). The precision decreases with decreasing CO_2 partial pressure, as the precision of pressure measurements decreases with a reduction in the pressure transient.

To test the validity of Equation (5), the mean values of $[(\partial P_t/\partial t)_{t=0}]$ for each set of experiments were plotted versus the relative partial pressures inside the cylinder (Figure 4). The data points define a linear trend, consistent with theoretical predictions. The obtained straight line can be used as calibration line, the angular coefficient of the straight line can be multiply by the values of $[(\partial P_t/\partial t)_{t=0}]$ for getting the CO_2 partial pressure values.

4. Concluding Remarks

We presented a simple methodology for measuring gas concentrations using a pressure transducer and a closed polymeric tube. We outlined the theoretical basis of the methodology, and performed experimental tests, using a tailor-made device, that demonstrated the validity of the proposed model. The tests also revealed the device's ability to measure a wide range of CO_2 partial pressures (0.032–0.89 atm) with good precision (< 6%). Under certain conditions, the device can be used for both single measurements and continuous monitoring in the field. The necessary conditions for such use are as follows: (i) a binary system consisting of monitored gases and a matrix of constant composition (e.g., air); (ii) if the matrix gases are not constant, the other species must have *Kp* values markedly different from those of the considered gases. In environments with characteristics highly similar to those discussed above and with conditions that are potentially damaging to existing instruments, the proposed device could represent a useful alternative for measuring CO_2 partial pressure. In our device, in fact, the gases are not required to be introduced into the sensor, and the electronic components (electrovalves, pump,

194 and pressure transducer) can be housed in a watertight box. In addition, the PTFE is very
195 resistant to acid gases. A common natural example of such an environment is soil, especially
196 soil located close to a fumarole field. Such areas occur at volcanoes throughout the world, and
197 are characterized by the presence of acid species, vapour flux, and a soil gaseous component
198 dominated by CO_2 and atmospheric gases, resulting from the condensation of fluids discharged
199 by the fumaroles [*Chiodini et al.*, 1996].

200 As a proof of concept this study shows that the proposed method can be used to measure
201 the concentration of CO_2 under the conditions outlined above. The variety of polymeric
202 materials available (e.g., polyetilene, polypropylene, PDMS), and the different properties of
203 gasses within them provide the potential for this method to be used in other systems apart from
204 the air/CO_2 system tested here.

205 **References**

206 Aiuppa, A., G. Giudice, S. Gurrieri, M. Liuzzo, M. Burton, T. Caltabiano, A. J. S. McGonigle,
207 G. Salerno, H. Shinohara, and M. Valenza (2008), Total volatile flux from Mount Etna,
208 *Geophys. Res. Lett., 35,* L24302, doi:10.1029/2008GL035871.

209 Barrer, R. M. (1934), Permeation diffusion and solution of gases in organic polymers, *Trans.*
210 *Faraday Soc*., *35*, 628–643.

211 Beaubien S.E., G. Ciotoli, and S. Lombardi (2003), Carbon dioxide and radon gas hazard in the
212 Alban Hills area (central Italy), *J. Volcanol. Geotherm. Res.123*, 63–80.

213 Capasso, G., M. L. Carapezza, C. Federico, S. Inguaggiato, and A. Rizzo (2005), Geochemical
214 monitoring of the 2002–2003 eruption at Stromboli volcano (Italy): precursory changes in
215 the carbon and helium isotopic composition of fumarole gases and thermal waters, *Bull.*
216 *Volcanol., 68,* 118–134.

217 Chiodini, G., F. Frondini, and B. Raco (1996), Diffuse emission of CO_2 from the Fossa crater,
218 Vulcano Island (Italy) *Bull. Volcanol., 58,* 41–50.

219 D'Alessandro, W., S. De Gregorio, G. Dongarrà, S. Gurrieri, F. Parello, and B. Parisi (1997),
220 Chemical and isotopic characterization of the gases of Mount Etna, *J. Volcanol.*
221 *Geotherm. Res., 78,* 65–76.

222 De Gregorio, S., S. Gurrieri, and M. Valenza (2005), A PTFE membrane for the in situ
223 extraction of dissolved gases in natural waters: Theory and applications, *Geochem.*
224 *Geophys. Geosyst.*, *6*, Q09005, doi:10.1029/2005GC000947.

225 Faber, E., Mora´ N., C., Poggenburg, j., Garza´ N., G., and Teschner, m. (2003), Continuous
226 gas monitoring at Galeras volcano, Colombia: first evidence, *J. Volcanol. Geotherm.*
227 *Res.,125(1–2),* 13–23.

228 Fischer, T. P., P. Burnard, B. Marty, D.R. Hilton, E. Füri, F. Palhol, Z.D. Sharp, and F.
229 Mangasini (2009), Upper-mantle volatile chemistry at Oldoinyo Lengai volcano and the
230 origin of carbonatites, *Nature 459*, 77–80.
231 Kana, T. M., C. Darkangelo, M. D. Hunt, J. B. Oldham, G. E. Bennett, and J. C. Cornwell
232 (1994), Membrane inlet mass spectrometer for rapid high-precision determination of N_2,
233 O_2, and Ar in environmental water samples, *Anal. Chem.*, *66*, 4166–4170.
234 Lupton, J., et al. (2006), Submarine venting of liquid carbon dioxide on a Mariana Arc volcano,
235 *Geochem. Geophys. Geosyst.*, *7*, Q08007, doi:10.1029/2005GC001152.
236 Scholes, C. A., S. E. Kentish, and G. W. Stevens (2008), Carbon Dioxide Separation through
237 Polymeric Membrane Systems for Flue Gas Applications. *Recent Patents on Chemical*
238 *Engineering*, *1*, 52–66.
239 Shinohara, H., A. Aiuppa, G. Giudice, S. Gurrieri, and M. Liuzzo (2008), Variation of
240 H_2O/CO_2 and CO_2/SO_2 ratios of volcanic gases discharged by continuous degassing of
241 Mount Etna volcano, Italy, *J. Geophys. Res.*, *113*, B09203, doi:10.1029/2007JB005185.
242 Takahata, N., G. Igarashi, and Y. Sano (1997), Continuous monitoring of dissolved gas
243 concentrations in groundwater using a quadrupole mass spectrometer, *Appl. Geochem. 12*,
244 377–382.
245 Tortell, P. D. (2005), Dissolved gas measurements in oceanic waters made by membrane inlet
246 mass spectrometry, *Limnol. Oceanogr.: Methods 3*, 24–37.
247 Wijmans, J. G., and R. W. Baker, (1995), The solution diffusion model: A review, *J. Membr.*
248 *Sci.*, *107*, 1–21.
249 Zhang, D., et al. (2008), Temporal and spatial variations of the atmospheric CO_2 concentration
250 in China, *Geophys. Res. Lett.*, *35*, L03801, doi:10.1029/2007GL032531.

251 Zimmer M., and J. Erzinger (2003), Continuous H_2O, CO_2, ^{222}Rn and temperature
252 measurements on Merapi Volcano, Indonesia, *J. Volcanol. Geotherm. Res.*, 125 (2003)
253 25–38.

Figure captions

Figure 1. Theoretical curves of temporal variations in P_t within a polymeric tube for four different values of $(P_{a2} - P_{in2})$. The values (in atm) are listed next to each curve. For the upper part of the graph, where $Kp_1 < Kp_2$, gas 2 permeates into the polymeric tube at a higher rate than does gas 1, resulting in a positive P_t pressure. For the lower part of the graph, where $Kp_1 > Kp_2$, a negative P_t transient is recorded. The most important result is that in both cases the P_t transient is proportional to $(P_{a2} - P_{in2})$.

Figure 2. Sketch of the experimental apparatus used in the tests. The PTFE tube is connected to two stainless-steel capillaries emerging from the top of the cylinder plug, where they are connected to a pump and two electrovalves.

Figure 3. Examples of temporal variations in experimental P_t values at eight different CO_2 partial pressures. The total pressure values are normalized to a starting pressure of 1 atm. The solid lines are the fitted five-degree polynomial functions.

Figure 4. Mean computed values of $[(\partial P_t/\partial t)_{t=0}]$ versus measured CO_2 partial pressures. The error bars for $[(\partial P_t/\partial t)_{t=0}]$ lie within the size of the symbols. The data points define a linear trend, as predicted by theoretical equations.

Table 1. Values of $[(\partial P_t/\partial t)_{t=0}]$[a] for every series and statistical parameters

CO_2 Partial pressure (atm)	0.032	0.10	0.24	0.33	0.53	0.60	0.76	0.89
Series								
1	1.31	3.74	9.40	13.59	21.30	24.01	30.63	36.55
2	1.18	3.70	9.35	13.22	21.18	24.29	30.44	36.97
3	1.24	3.97	9.34	13.59	20.82	24.09	30.13	36.63
4	1.19	3.67	9.11	14.12	20.79	24.10	30.24	37.00
5	1.12	3.88	9.01	13.36	21.04	24.00	30.34	36.99
6	1.20	3.81	8.75	13.38	20.90	23.79	30.03	36.93
7	1.22	3.52	9.43	13.43	20.86	24.45	29.92	36.78
8	1.30	3.66	9.56	13.41	20.97	24.05	30.07	36.41
9	1.28	3.77	9.27	13.41	20.75	24.01	30.20	36.73
10	1.10	3.88	9.15	13.25	20.71	23.75	30.33	36.83
Mean value[a]	**1.21**	**3.76**	**9.24**	**13.48**	**20.93**	**24.05**	**30.23**	**36.78**
Uncertainty[a]	**0.07**	**0.13**	**0.24**	**0.26**	**0.20**	**0.21**	**0.22**	**0.20**
Precision (%)	**5.9**	**3.5**	**2.6**	**1.9**	**1.0**	**0.9**	**0.7**	**0.6**

[a]The original values (atm sec^{-1}) were multiplied by 10^5 for presentation in the table.

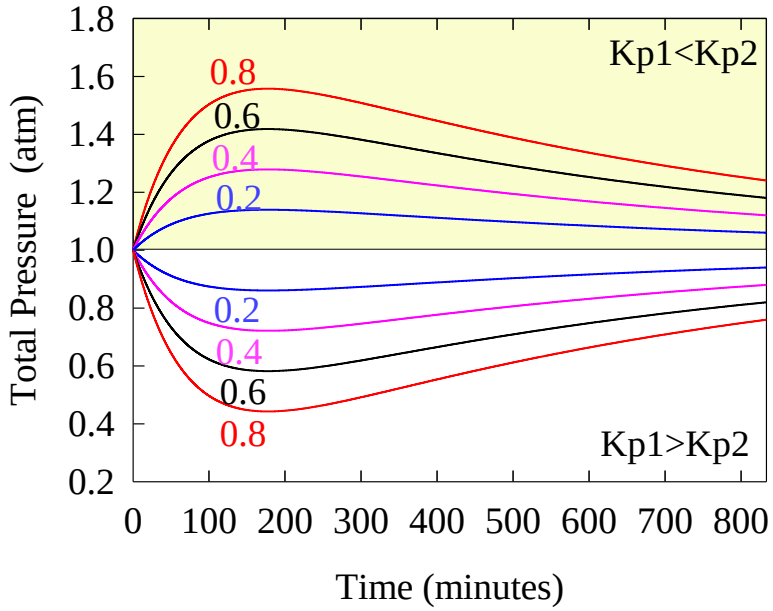
Total Pressure (atm)
Time (minutes)
Kp1<Kp2
Kp1>Kp2
0.8
0.6
0.4
0.2
0.2
0.4
0.6
0.8
1.8
1.6
1.4
1.2
1.0
0.8
0.6
0.4
0.2
0
100
200
300
400
500
600
700
800

Figure 1.

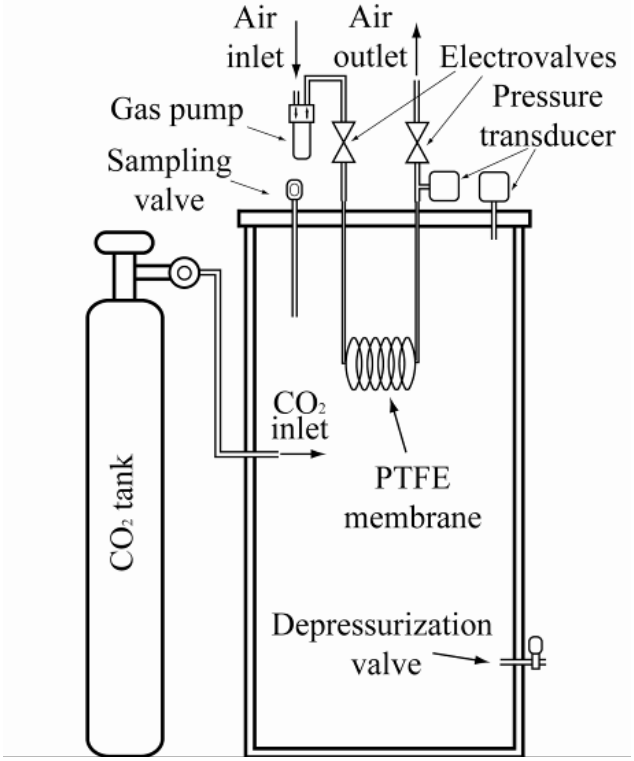
Air
inlet
Air
outlet
Electrovalves
Pressure
transducer
Gas pump
Sampling
valve
CO2
inlet
PTFE
membrane
CO2 tank
Depressurization
valve

Figure 2.

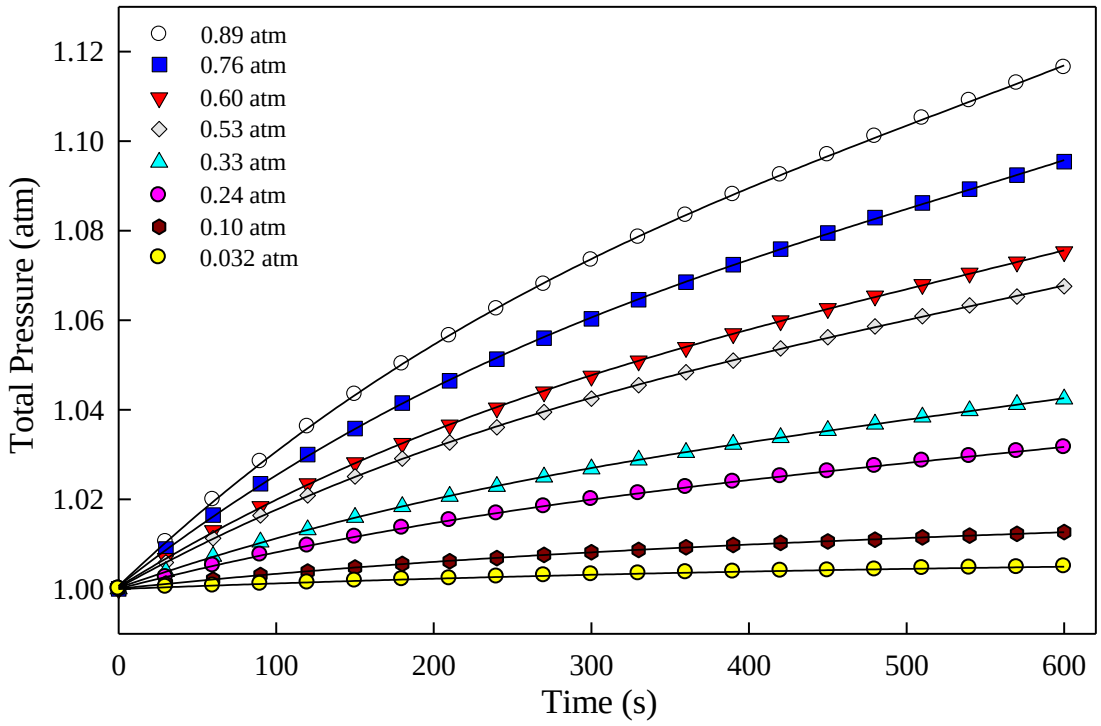
0.89 atm
0.76 atm
0.60 atm
0.53 atm
0.33 atm
0.24 atm
0.10 atm
0.032 atm
Total Pressure (atm)
1.12
1.10
1.08
1.06
1.04
1.02
1.00
0
100
200
300
400
500
600
Time (s)

Figure 3.

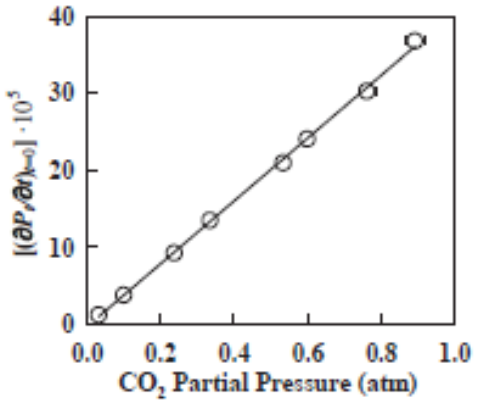
40
30
20
10
0
0.0
0.2
0.4
0.6
0.8
1.0
$[(\partial P_r/\partial r)_{r=0}] \cdot 10^3$
CO_2 Partial Pressure (atm)

Figure 4